
From Anatomic Standardization Analysis of Perfusion SPECT Data to Perfusion Pattern Modeling:

Evidence of Functional Networks in Healthy Subjects and Temporal Lobe Epilepsy Patients¹

Christophe Grova, PhD, Pierre Jannin, PhD, Irène Buvat, PhD, Habib Benali, PhD, Jean-Yves Bansard, PhD, Arnaud Biraben, MD, Bernard Gibaud, PhD

Rationale and Objectives. In the general context of perfusion pattern modeling from single-photon emission computed tomographic (SPECT) data, the purpose of this study is to characterize interindividual functional variability and functional connectivity between anatomic structures in a set of SPECT data acquired from a homogeneous population of subjects.

Materials and Methods. From volume of interest (VOI)-perfusion measurements performed on anatomically standardized SPECT data, we proposed to use correspondence analysis (CA) and hierarchical clustering (HC) to explore the structure of statistical dependencies among these measurements. The method was applied to study the perfusion pattern in two populations of subjects; namely, SPECT data from 27 healthy subjects and ictal SPECT data from 10 patients with mesio-temporal lobe epilepsy (MTLE).

Results. For healthy subjects, anatomic structures showing statistically dependent perfusion patterns were classified into four groups; namely, temporomesial structures, internal structures, posterior structures, and remaining cortex. For patients with MTLE, they were classified as temporomesial structures, surrounding temporal structures, internal structures, and remaining cortex. Anatomic structures of each group showed similar perfusion behavior so that they may be functionally connected and may belong to the same network. Our main result is that the temporal pole and lenticular nucleus seemed to be highly relevant to characterize ictal perfusion in patients with MTLE. This exploratory analysis suggests that a network involving temporal structures, lenticular nucleus, brainstem, and cerebellum seems to be involved during MTLE seizures.

Conclusion. CA followed by HC is a promising approach to explore brain perfusion patterns from SPECT VOI measurements.

Key Words. Functional variability; single-photon emission computed tomography (SPECT); correspondence analysis (CA); hierarchical clustering (HC); mesio-temporal lobe epilepsy; ictal perfusion.

© AUR, 2005

Acad Radiol 2005; 12:554–565

¹ From Laboratoire IDM Medical School, University of Rennes 1, 35043 Rennes Cedex, France (C.G., P.J., A.B., B.G.) and INSERM U642, University of Rennes 1, 35043 Rennes Cedex (J.-Y.B.); UMR 678 INSERM/UPMC, Laboratoire d'Imagerie Fonctionnelle, Pitié Salpêtrière, Paris, France (I.B., H.B.). Received July 24, 2004; Accepted August 17. This work was supported in part by a grant from the Conseil Régional de Bretagne. **Address correspondence to:** C.G. ²Current address: Montreal Neurological Institute, McGill University, Montreal, 3801 University Street, EEG department, Room 028, Montreal, Quebec, Canada, H3A 2B4. e-mail: christophe.grova@mail.mcgill.ca

© AUR, 2005

doi:10.1016/j.acra.2004.08.014

Single-photon emission computed tomography (SPECT) using technetium 99m (^{99m}Tc)-hexylmethyl-propylene-amine oxime (HMPAO) or ^{99m}Tc-ethylcysteinatedimer (ECD) as a radiotracer is the most widely applied technique to study cerebral blood flow (1). Ictal SPECT is a high-sensitive technique for imaging extreme perfusion changes occurring during an epileptic seizure (2). It provides valuable information for the presurgical investigation of epilepsy. A perfusion pattern is defined as a typical spatial organization of brain perfusion in a homogeneous set of SPECT data. Perfusion patterns may be used to characterize subtypes of a pathological state, for example, in temporal lobe epilepsy

(3,4). Characterizing brain perfusion interindividual functional variability in SPECT is a key issue to better understand physiological and physiopathological characteristics, study functional connectivity, support diagnosis, and derive a model for perfusion pattern. Volume of interest (VOI)-based anatomic standardization analysis has been used widely to study normal perfusion patterns in SPECT (5–7). Such methods rely on an a priori spatial model of brain anatomy described by VOI definition. VOI-based analysis assumes that the perfusion values of interest are homogeneous within each VOI. The main perfusion models reported in the literature reflected mainly interindividual average perfusion characteristics (see [6] for a study of 89 healthy subjects). We previously proposed a spatial model of brain anatomy, ie, VOIs, dedicated to the analysis of ictal SPECT data for patients with mesio-temporal lobe epilepsy (MTLE) (8). Such an anatomic model was used to create an average model for normal perfusion within healthy subjects and an average model for ictal perfusion in patients with MTLE.

Analyzing interindividual functional variability of brain perfusion within a set of SPECT data is needed for perfusion pattern modeling. Principal component analysis of SPECT data sets already has been proposed to study functional variability within a population of healthy subjects (7,9) or a population of patients with temporal lobe epilepsy (10). Those methods aim to identify anatomic structures in which perfusion is covarying between subjects of a same homogeneous group. Discriminant analysis has been used for nonsupervised classification between normal and pathological SPECT data (11). Characterization of a perfusion pattern may be achieved by studying “dependencies” between anatomic structures (eg, correlation, statistical dependencies, or functional connectivity). This aspect is of particular interest in the context of the presurgical investigation of epilepsy, especially because the notion of an epileptogenic network seems helpful to better understand epilepsy (12,13). Concerning ictal SPECT in patients with temporal lobe epilepsy, evidence of underlying functional networks involving the thalamus, basal ganglia, and cerebellum already was suggested (10,14,15).

The purpose of this study is to propose a new method to characterize interindividual functional variability and statistical dependencies between anatomic structures from SPECT data. We combined correspondence analysis (CA) and ascending hierarchical clustering (HC) (16) to explore perfusion patterns observed using SPECT data sets acquired from a homogeneous population of subjects. By combining both approaches, we were able to extract the

most meaningful information from the data by using CA, then identify groups of anatomic structures showing similar perfusion behavior by using HC. This multivariate analysis was performed on VOI measurements obtained after anatomic standardization, as proposed in Grova et al (8). Perfusion patterns were studied from normal SPECT data of 27 healthy subjects and ictal SPECT data of 10 patients with MTLE.

MATERIAL AND METHODS

Anatomic Standardization Analysis

Spatial model of brain anatomy.—VOI selection was deduced from the anthropomorphic model of the head proposed by Zubal et al (17). This model was established from T1-weighted high-resolution three-dimensional (3D) magnetic resonance imaging (MRI) of a healthy subject from which VOIs were hand drawn and labeled. To generate a spatial model of brain anatomy appropriate to study perfusion patterns seen in patients with temporal lobe epilepsy (3), temporal and frontal VOIs of Zubal phantom were resegmented into their mesial, lateral, and polar components. To study perfusion interhemispheric asymmetries, all VOIs were relabeled as belonging to the right or left hemisphere. Fifty-two lateralized brain VOIs thus were generated from Zubal phantom.

Population of subjects, data acquisition, and preprocessing.—Two populations of subjects showing characteristic perfusion patterns were considered. SPECT scans of 27 healthy subjects (12 men, 15 women; age, 20–56 years) were used to study normal perfusion. These data were provided by Dr Barnden from the Queen Elizabeth Hospital (Woodville, Australia). Ictal SPECT from 10 patients with MTLE (six men, four women; age, 19–43 years) from the Rennes University Hospital (Rennes, France) were selected to derive a model of ictal perfusion. Patient selection was based on both clinical data and results of surgery. Clinical data showed the usual temporal ictal semiology (cf epigastric sensation, dreamy state, and automatism), absence of secondary generalization in their history, and unilateral involvement of the temporal lobe on electroencephalography (EEG). Ictal SPECT data thus showed a typical ictal perfusion pattern for MTLE, as described in (3). After clinical investigations including SPECT acquisitions, all patients with MTLE underwent curative surgery and are now seizure free (Engel class Ia [18]). The pathological hemisphere then was clearly identified for each patient.

For 27 healthy subjects, SPECT images were acquired by using a three-head gamma camera equipped with ultrahigh-resolution parallel collimators (IRIX; Philips Medical Systems, Cleveland, OH) after injection of 500 MBq of ^{99m}Tc -HMPAO (120 projections over 360° ; 128×128 matrix; pixel size, 3.59 mm). For 10 patients with MTLE, ictal SPECT images were acquired by using a two-head DST-XL camera (General Electric Medical Systems, Buc, France) equipped with fan beam or parallel ultrahigh-resolution collimators (64 projections over 360° ; 128×128 matrix; pixel size, 4.51 mm). ^{99m}Tc -HMPAO, 740 MBq, was injected 52 ± 15.3 (SD) seconds after the onset of the seizure, relying on EEG measurements (seizure duration, 92 ± 23.3 seconds).

All SPECT data were reconstructed by using filtered back-projection with a ramp filter (Nyquist frequency cut-off). Reconstructed data were postfiltered with an 8-mm full-width at half-maximum (FWHM) 3D Gaussian filter. Spatial resolution was FWHM of 12.2 mm for all reconstructed images. Scatter correction was performed only for healthy subjects using the method of Jaszczak et al (19) by subtracting projections corresponding to a simultaneous acquired Compton window. No simultaneous acquisition in a Compton window was available for retrospective ictal SPECT data. Assuming uniform attenuation in the head, first-order Chang (20) attenuation correction was performed, with attenuation coefficients of $\mu = 0.15 \text{ cm}^{-1}$ for scatter-corrected data and $\mu = 0.12 \text{ cm}^{-1}$ for uncorrected data (19).

Spatial normalization.—To perform SPECT measurements in VOIs of the spatial model (see *Spatial model of brain anatomy*), we used the spatial normalization method described by Friston et al (21) and implemented in the Statistical Parametric Mapping (SPM99; <http://www.fil.ion.ucl.ac.uk/spm/>) software. SPECT data and VOIs of the spatial model were both spatially normalized to a mean anatomic reference volume, represented by the T1 template provided by SPM, as follows:

1. A nonlinear geometric transformation was estimated to match the 3D T1-weighted MRI of the Zubal phantom, and thus VOIs, on the T1 SPM template.
2. For 27 healthy subjects, SPECT images were spatially normalized to the SPECT template provided by SPM by using an affine geometric transformation, as recommended by Acton and Friston (22); the SPECT SPM template is by construction in the same referential as the T1 SPM template.
3. For 10 patients with MTLE, a two-step approach

was used to achieve spatial normalization of ictal SPECT data, which showed large hyperperfused areas. First, an intermodality/inpatient rigid registration was performed between each patient's ictal SPECT and MRI data by maximization of mutual information (23). Each subject's 3D T1-weighted MRI then was spatially normalized to the T1 SPM template by using a nonlinear geometric transformation.

All these linear or nonlinear geometric transformations allowed resampling of the SPECT data and VOIs in the unique mean anatomic reference, ie, the T1 SPM template, by using trilinear interpolation. Spatial normalization was checked visually by a neurosurgeon by superimposing each SPECT, MRI, and VOI resampled in this mean anatomic reference volume (Figure 1). No significant deformation errors were detected visually.

Perfusion measurements and intensity normalization.—For each VOI j and each SPECT data set i , a perfusion measurement consisted of the estimation of the mean SPECT intensity x_{ij} within the VOI. To remove the confounding effect of global interacquisition changes in SPECT, each measurement was normalized in intensity so that mean voxel count throughout the brain was approximately 50 counts/voxel.

Perfusion Pattern Modeling

Whereas average perfusion models deduced from those VOI measurements were proposed in (8), the purpose of this study is to provide a more detailed analysis of the underlying distribution of those perfusion measurements. Functional variability was explored by analyzing the structure of statistical dependencies between perfusion measurements. Considering VOIs and SPECT data sets as two qualitative variables, we applied CA followed by HC to study statistical dependencies between those variables (16).

Correspondence Analysis (CA) and Ascending Hierarchical Clustering (HC)

Generation of the contingency table.—CA relies on the analysis of a contingency table N , where each element n_{ij} describes the number of observed individuals partitioned among the modalities i and j of two qualitative variables. In our study, the two qualitative variables were the anatomical entities, ie, VOIs, and SPECT data sets. More precisely, to emphasize interhemispheric asymmetries dur-

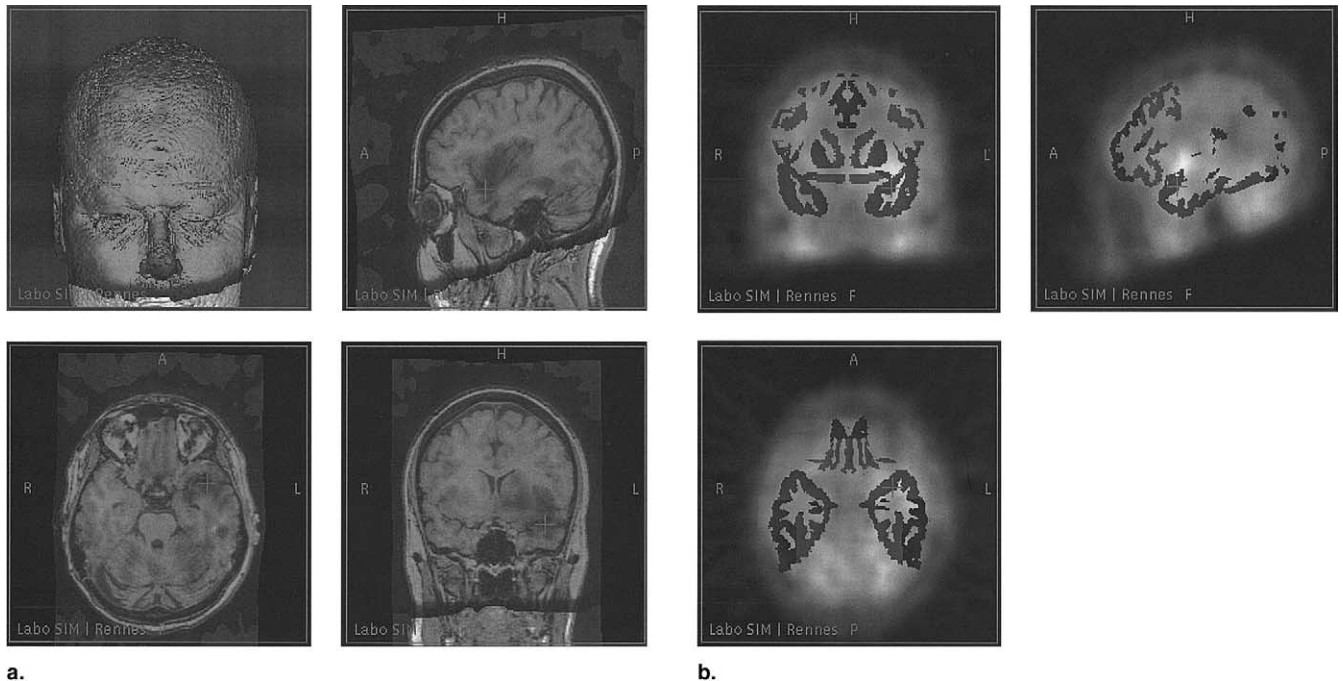


Figure 1. Multimodal data fusion for SPECT anatomic standardization analysis: **(a)** ictal SPECT of a patient with epilepsy superimposed on its MRI, both spatially normalized to the SPM T1 template; and **(b)** frontal, temporal, and some internal VOIs of the spatial model superimposed on the spatially normalized ictal SPECT of the same patient.

ing the analysis, we considered measurements from both hemispheres as two realizations of the same qualitative variable. The variable VOI_{nonlat} thus described the name of the nonlateralized VOIs of our spatial model, whereas the variable $Subject_{Hem}$ characterized the “name” of the measured hemisphere of each subject. We distinguished left versus right hemispheres for healthy subjects and ipsilateral versus contralateral hemispheres with respect to the epileptogenic focus for patients with MTLE. The variable $Subject_{Hem}$ is described by $m1 = 2 \times 27 = 54$ modalities for healthy subjects ($m1 = 2 \times 10 = 20$ modalities for MTLE patients). VOI_{nonlat} is described by $m2 = 52/2 = 26$ anatomical entities. A contingency table N was generated by assigning the corresponding measurement x_{ij} (cf *Perfusion measurements and intensity normalization*) to each pair of $Subject_{Hem}$ and VOI_{nonlat} modalities.

Basics of CA estimates.—From a contingency table N described by $m1$ rows and $m2$ columns, CA estimates relationships between distribution profiles; namely, relationships between row profiles or column profiles. A row profile i is defined by n_{ij}/n_i for: $j \in \langle 1, m2 \rangle$ where n_i is the i^{th} row sum. It represents the percentage of perfusion value stored in each VOI_{nonlat} for a particular $Subject_{Hem}$. A row profile also may be considered as an individual (ie, a modality of $Subject_{Hem}$) described by $m2$ variables (ie,

modalities of VOI_{nonlat}). Similarly, a column profile j defined by n_{ij}/n_j for: $i \in \langle 1, m1 \rangle$ n_j being the j^{th} column sum, is the percentage of perfusion value stored in each $Subject_{Hem}$ for a particular VOI_{nonlat} .

CA provides a multivariate analysis of the distribution shapes of those profiles (row or column) independent from the intensity of perfusion values. Similarities between profiles are taken into account by using a χ^2 metric. The χ^2 -distance between two row profiles i and i' is defined by:

$$d(i, i')^2 = \sum_{j=1}^{m2} \frac{1}{n_{.j}} \left(\frac{n_{ij}}{n_i} - \frac{n_{i'j}}{n_{i'}} \right)^2 \tag{3}$$

The χ^2 -distance between two column profiles is defined similarly. CA may then be interpreted as a principal component analysis (PCA) of those row profiles (or column profiles) by using the χ^2 distance as a metric. The χ^2 distance is a well-known similarity measure of statistical dependence between qualitative variables. Such metric makes it possible to compare shapes of distribution profiles, providing an analysis of the underlying structure of statistical dependencies among modalities of VOI_{nonlat} and $Subject_{Hem}$.

A threshold on the decreasing eigenvalues resulting from CA is applied to select the subspace containing the most meaningful information. Variables, ie, column profiles VOI_{nonlat} , and individuals, ie, row profiles $Subject_{Hem}$, then were represented by their projections on the first principal components.

Interpretation of results of CA using HC.—Within the subspace selected by CA associated with the Euclidian distance, we applied ascending HC on CA principal components to extract groups of variables VOI_{nonlat} or individuals $Subject_{Hem}$ considered as neighbors. Using the Ward criterion to aggregate similar clusters at each level of HC (16), we obtained a classification tree of neighbor “points,” ie, variables or individuals. “Cutting” the tree then provided classification of those points. Points belonging to the same cluster were considered statistically dependent. Conversely, points located in different clusters were considered closer to independence.

To help interpretation, the center of mass of each cluster of anatomic structures VOI_{nonlat} was projected on the two first principal components. The square cosine of the angle between each center of mass and its projection on each principal component was assessed to evaluate the quality of the representation. All statistical analyses were performed using R software (<http://www.r-project.org/>).

RESULTS

Analysis of Perfusion Measurements in Healthy Subjects

Projection of variables on the first two principal components is shown in Figure 2a. The first two principal components corresponded to 34.3% of global inertia. For HC, we selected the first five principal components, accounting for 67.5% of global inertia. By cutting the classification tree presented in Figure 2b, HC allowed us to distinguish four groups of anatomic structures:

1. Internal structures: thalamus (contribution of 30.1% to the second principal component), caudate nucleus (contribution of 16.8% to the second principal component), basal ganglia (contribution of 12.5% to the second principal component), and lenticular nucleus
2. Temporomesial structures: amygdala (contribution of 49.7% to the first principal component and 12.4% to the second), hippocampus, and temporal pole
3. Posterior structures: inside (occipital, occipitolateral,

and occipitomesial) and outside the cerebral cortex (cerebellum and brainstem)

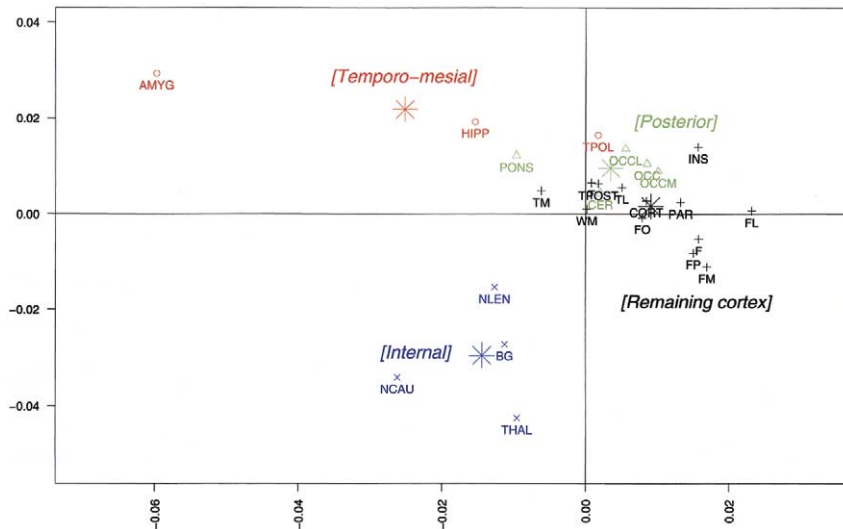
4. Remaining cortex.

In each case, we indicated the structures presenting the greatest contributions to the inertia projected on the first two principal components. This analysis showed that the structure of statistical dependencies between anatomic structures for normal perfusion was complex because it clearly required more than two principal components to be characterized accurately. Projections on the first two principal components presented in Figure 2a thus may be misleading. For all clusters except the posterior structure one, the center of mass of the cluster was represented accurately on the first two principal components, showing high square cosines (Table 1). The cluster posterior structures was represented better on the third and fourth principal components, and its projection close to the cluster remaining cortex on the first two principal components (cf Figure 2a) is misleading. These four groups of statistically dependent anatomic structures, extracted by means of HC by using five principal components, seemed highly relevant to characterize the normal perfusion pattern. Conversely, analysis of the individuals $Subject_{Hem}$ was not really informative on this population (results not shown).

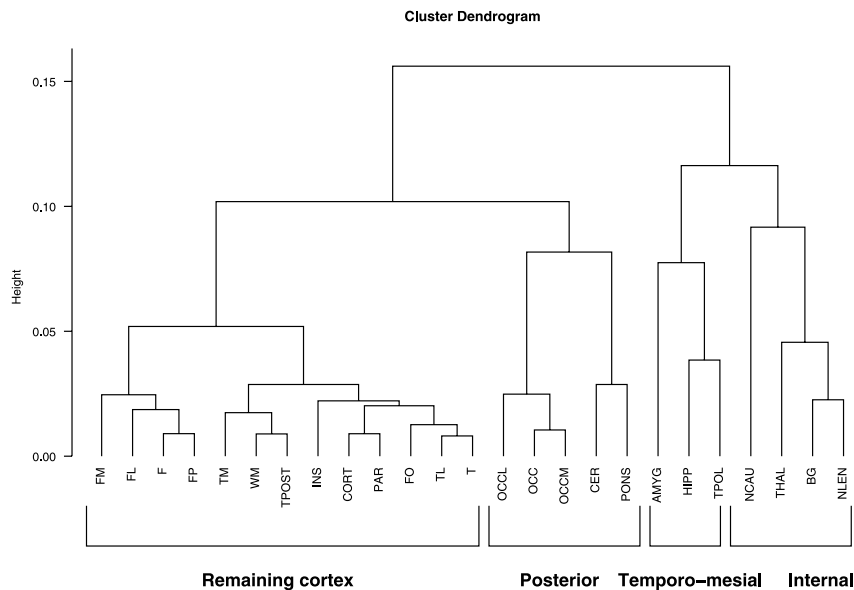
Analysis of Ictal Perfusion Measurements in Patients With MTLE

The first two principal components were considered sufficient to extract the main information (69.2% of global inertia) from the analysis of ictal SPECT of 10 patients with MTLE. Figure 3a shows the projection of variables on those first two principal axes. Similarly to the healthy subject analysis, HC within the selected subspace yielded four groups of statistically dependent anatomic structures, shown in Figure 3a and b:

1. Temporomesial structures: temporal pole (contribution of 21.3% to the first principal component), amygdala (contribution of 15.8% to the first principal component), and hippocampus
2. Surrounding temporal structures: temporomesial, temporolateral, temporal, orbitofrontal, insula, and lenticular nucleus, also including some posterior structures outside the cerebral cortex, such as cerebellum and brainstem
3. Internal structures: thalamus (contribution of 38.0% to the second principal component), caudate nucleus



a.



b.

Figure 2. Analysis of SPECT data from 27 healthy subjects: **(a)** projection of variables (VOI_{nonlat}) on the first two principal components and **(b)** classification tree obtained by means of HC after CA using five components. Several clusters of anatomical structures were extracted from HC and are indicated on the dendrograms **(b)**; namely, *temporomesial structures* (red o), *internal structures* (blue x), *posterior structures* (green Δ), and *remaining cortex* (black +). The center of mass of each cluster (*) was projected on the first two principal components, and the corresponding name of the cluster is shown using the same color code and italic font. Note that better discrimination between posterior structures and the remaining cortex clusters in **(a)** was observed on the third principal component. CORT, cortex; WM, white matter; AMYG, amygdala; HIPP, hippocampus; NCAU, caudate nucleus; BG, basal ganglia; NLEN, lenticular nucleus; THAL, thalamus; INS, insula; T, temporal; TPOL, temporal pole; TM, temporal mesial; TL, temporal lateral; TPOST, temporal posterior; F, frontal; FP, frontal pole; FO, orbito frontal; FM, frontal mesial; FL, frontal lateral; OCC, occipital; OCCM, occipital mesial; OCCL, occipital lateral; PAR, parietal; CER, cerebellum; PONS, brainstem.

(contribution of 21.7% to the second principal component), and basal ganglia

4. Remaining cortex.

The centers of mass of all those clusters were represented accurately on the first two principal components, showing high square cosines (Table 1). The first principal component represented mainly the temporomesial versus remaining cortex clusters, whereas the second principal component represented mainly the surrounding temporal versus internal structure clusters. Compared with the analysis of healthy subjects, we observed a similar distinction between temporomesial structures, internal structures, and remaining cortex. Nevertheless, some differences between normal and ictal perfusion patterns were observed. The lenticular nucleus VOI belonging to the group of internal structures for the healthy subject analysis was assigned to the group of surrounding temporal structures, ie, close to the pathological area. Although the temporal-pole VOI was classified within the temporomesial cluster for both analyses, it has greater influence on the ictal perfusion pattern, showing a greater contribution to the first principal component (21.1%). The anatomic structures temporal pole and lenticular nucleus thus seemed very relevant to describe the ictal perfusion pattern seen during MTLE

Table 1
Square Cosines of the Angle Between the Center of Mass of Each Cluster of VOI_{nonlat} and Its Projection on the Selected Principal Components

HC performed on healthy subjects					
Cluster name	Principal component				
	1st	2nd	3 rd	4th	5th
[Internal structures]	0.18	0.76	0.02	0.01	0.00
[Temporo-mesial]	0.41	0.30	0.10	0.07	0.06
[Posterior]	0.02	0.14	0.45	0.24	0.02
[Remaining cortex]	0.63	0.02	0.02	0.10	0.00
HC performed on MTLE patients					
	1st	2nd			
[Internal structures]	0.11	0.87			
[Temporo-mesial]	0.92	0.04			
[Surrounding temporal]	0.14	0.69			
[Remaining cortex]	0.98	0.00			

Note. Principal components on which clusters were better represented (ie, smallest angles or highest square cosines) are presented in bold.

HC, hierarchical clustering; MTLE, mesio-temporal lobe epilepsy.

seizures. Note that the cerebellum and brainstem also were associated with the surrounding temporal cluster, whereas occipital areas now were classified within the remaining cortex group. The dual representation showing the projection of individuals on the first two principal components, shown in Figure 4, highlights a relevant discrimination between hemispheres ipsilateral and contralateral to the epileptogenic focus.

DISCUSSION

We proposed to combine CA and ascending HC to explore statistical dependencies among perfusion measurements performed using VOIs applied on anatomically standardized SPECT data. The method was used to study normal perfusion measured in 27 healthy subjects and ictal perfusion as seen in 10 patients with MTLE. For both groups, we found relevant structures of statistical dependencies between perfusion measurements, suggesting that CA associated with HC is a promising approach to characterize functional variability among SPECT data sets acquired from a homogeneous population. By using CA, our approach differed from previously reported studies using PCA (7,9,10). CA theoretically extracts more general links between variables than PCA because it explores statistical dependencies between the shapes of perfusion measurement profiles by using the χ^2 metric, whereas PCA assumes that distributions of perfusion measurements are Gaussian and explores correlations between the intensity of perfusion values. Moreover, whereas both CA and PCA aim at extracting the most meaningful information from the data and removing the noise, our main contribution was to use HC to assist the interpretation of results of CA and find some features that can characterize the perfusion pattern. HC performed on the subspace selected by CA allowed us to identify groups of anatomical structures "statistically dependent," ie, showing similar perfusion behavior within the population. HC particularly was needed when characterizing complex statistical dependencies, which requires more than two principal components. For example, in the case of the normal perfusion pattern, five principal components were necessary to describe the pattern.

Although groups of statistically dependent anatomical structures were clearly shown from the analysis of both healthy subjects and patients with MTLE, our results should be interpreted with caution, especially because of the limited number of SPECT studies. In addition, the

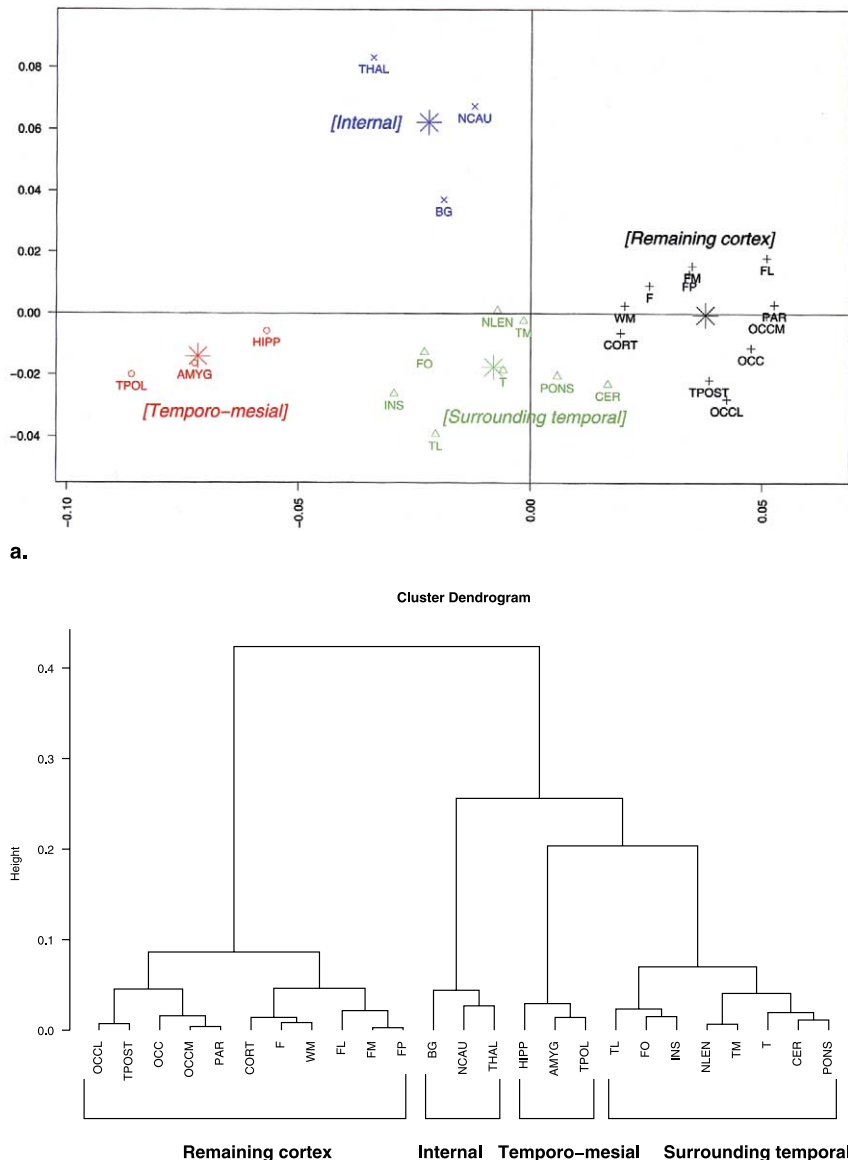


Figure 3. Analysis of ictal SPECT data from 10 patients with MTLE: **(a)** projection of the variables (VOI_{nonlat}) on the first two principal components and **(b)** classification tree obtained by means of HC after CA using 2 components. Several clusters of anatomical structures were extracted from HC and are indicated on the dendrograms **(b)**; namely, *temporomesial structures* (red o), *surrounding temporal structures* (green Δ), *internal structures* (blue x), and *remaining cortex* (black +). The center of mass of each cluster (*) was projected on the first two principal components, and the corresponding name of the cluster is shown using the same color code and italic font. Note that the temporal pole VOI is highly relevant to characterize the *temporomesial* cluster, whereas perfusion of the lenticular nucleus, brainstem, and cerebellum is associated with the *surrounding temporal* cluster. Anatomical structure abbreviations in Figure 2.

proposed analysis may be spoiled by quantification errors caused by the spatial normalization step or perfusion measurement step. Those errors thus may artificially generate statistical dependencies between some perfusion measure-

ments. Because spatial resolution greatly affects the spatial range of statistical dependency between neighboring regions, we only considered reconstructed images with similar spatial resolution (ie, FWHM = 12.2 mm). Differ-

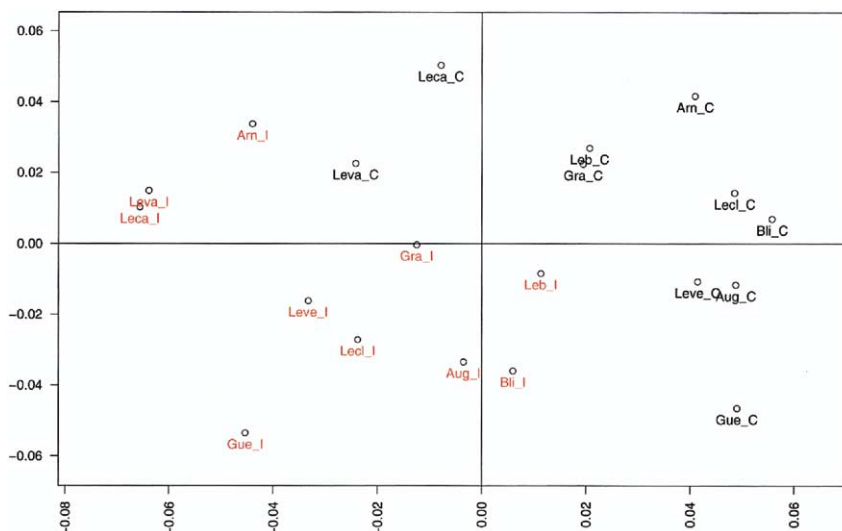


Figure 4. Projection of the individual ($Subject_{Hem}$) on the first two principal components for CA performed on ictal data of 10 patients with MTLE. ###_I (red) and ###_C (black) state for the hemispheres ipsilateral and contralateral to the epileptogenic focus for the corresponding patient ###, respectively. Note that clear discrimination between ipsilateral and contralateral hemispheres was observed.

ences in dependencies seen between the two groups therefore are unlikely to be caused by differences in spatial resolution. Moreover, because CA and HC performed on healthy subjects before and after scatter correction led to similar results (results not shown), scatter can be assumed not to affect the structure of statistical dependencies between regions.

Partial volume effect (PVE) caused by SPECT limited spatial resolution is the main source of absolute quantification errors within small structures in SPECT (eg, [24]). It may explain some statistical dependencies between small neighboring VOIs. We may assume that main dependencies between distant anatomical structures were preserved, although data were not corrected for PVE. Our results are in agreement with previous studies performed without PVE correction that reported functional variability within healthy subjects (7,9) or underlying networks in patients with MTLE (10,14,15). Even if VOI-based or voxel-based methods to correct for PVE have been proposed and validated on positron emission tomography (PET) (25) and SPECT data (24,26), achieving accurate PVE correction has never been shown on perfusion SPECT using a large number of VOIs, as in our study.

VOI-based perfusion measurements also may be biased by some errors arising from the spatial normalization step. However, the spatial normalization method we used to compensate for interindividual anatomical

variability (21) proved to be very accurate when applied to T1-weighted anatomical MRI, especially to preserve sulcogryal morphology (27). Because SPECT hypoperfusion areas were proved to decrease the accuracy of nonlinear spatial normalization (22,28), we assume that similar effects should happen with ictal SPECT showing large hyperperfused areas. We thus proposed a two-step approach (8) to spatially normalize ictal SPECT data by using first an ictal SPECT/MRI rigid registration that we validated in (29), followed by a nonlinear spatial normalization of the T1-weighted MRI. Because of the spatial normalization step and low spatial resolution of SPECT images, we assumed in the present study that anatomical interindividual variability had a negligible impact on the analysis of functional variability. However, we plan to investigate atlas-based segmentation methods, as proposed by Collins et al (30), to define VOIs directly on the MRI of each subject. Accurate VOI segmentation on each subjects' MRI will notably be particularly needed to correct for PVE.

Our results in 27 healthy subjects corroborate other studies exploring SPECT functional variability in a population of healthy subjects (6,7,9). Five principal components were needed to characterize the structure of statistical dependencies between VOIs. This complexity of the structure of normal perfusion is in agreement with previous observations, which highlighted the

significant effect of various parameters (eg, age, sex, laterality) on perfusion values (6,7). HC allowed us to select four groups of structures considered relevant to describe normal perfusion patterns; namely, internal structures, temporomesial structures, posterior structures, and remaining cortex. Perfusion within the posterior structure cluster, constituted by regions located both in (ie, occipital cortex) and outside (ie, brainstem and cerebellum) the cerebral cortex, thus was found to be relatively independent from the other clusters. Similar clusters of correlated anatomical structures already were reported by Pagani et al (7) by applying PCA on VOI-based perfusion measurements from 50 healthy subjects. However, 12 principal components were considered in (7) to explain 81% of the variance, whereas in our data, a similar percentage of global inertia could be explained by using eight principal components. Differences between these two studies may be explained in part by different acquisition and postprocessing protocols and the choice of the population of healthy subjects. Special attention must be given regarding selection of the population of healthy subjects when studying normal perfusion in SPECT (6).

Ictal SPECT data selected for this study were chosen to show a characteristic ictal perfusion pattern, as seen in patients with MTLE (3). Because of extreme perfusion changes caused by epileptic seizure, CA and HC show, as expected, clear discrimination between hemispheres ipsilateral and contralateral to the epileptogenic focus. The structure of statistical dependencies in ictal perfusion measurements was described completely by only the first two principal components, therefore being described more easily by our analysis than the normal perfusion pattern. The overall structure of statistical dependencies was concordant between ictal and normal perfusion measurements because similar clusters were identified by using HC. However, there was some difference because we identified no posterior structure group, but rather a surrounding temporal structure group that included some temporal structures, as well as orbitofrontal, insula, lenticular nucleus, cerebellum, and brainstem structures. Compared with the normal perfusion pattern, the VOIs temporal pole and lenticular nucleus were found to be highly relevant to characterize this ictal perfusion pattern. Using PCA on VOI measurements on ictal SPECT, Blumenfeld et al (10) found some correlations between similar anatomical structures in patients with temporal lobe epilepsy and proposed a model of the underlying network. Us-

ing HC, we propose a quantitative method to extract such a network from results of most significant dependencies selected by CA or PCA.

Other SPECT studies showed the implication of basal ganglia or cerebellum in ictal perfusion of patients with MTLE (10,14,15,31). These results and ours suggest the existence of an underlying network involving temporal structures, internal structures, brainstem, and the cerebellum during a seizure assessed by means of ictal SPECT. Evidence of such networks also was found in other functional studies. In interictal fluorodeoxyglucose (FDG) PET of patients with temporal lobe epilepsy, four hypometabolism patterns were found and confirmed by electrophysiological results (surface or depth recordings) (4). Basal ganglia, as well as the insula, were involved in those patterns, suggesting that interictal hypometabolism may be related to the ictal discharge generation and some spreading pathways. PET hypometabolism in basal ganglia, including lenticular nucleus, also was associated with the generation of dystonic postures occurring during a temporal seizure (32). Conversely, dystonia was associated with ictal SPECT hyperperfusion in the same structures (31). Finally, good agreement between metabolic patterns in FDG PET and ictal perfusion patterns in SPECT in patients with temporal lobe epilepsy was reported in (33), emphasizing the key role of the temporal pole. In structural image study and EEG, the role of the temporal pole in patients with MTLE is an interesting open question (cf a special issue of *Epileptic Disorders* [34]). MRI findings of more diffuse temporal lobe atrophy including the temporal poles (35), as well as depth EEG abnormalities arising from these regions (36), suggest that the temporal pole is clearly involved in MTLE seizures.

The existence of anatomical pathways involving temporal lobes and subcortical structures is well known, and epileptic seizures may involve widespread network interactions between cortical and subcortical structures (10,37). Although it may be more difficult to electrophysiologically implicate the cerebellum with seizures, there is no doubt regarding its pathological involvement in epilepsy. Whether it is affected secondarily by the seizures themselves, by the antiepileptic drug used, or by the underlying epileptogenicity remains unclear. According to our results, CA and HC thus seem to be a promising approach to explore statistical dependencies among temporal, internal, and posterior structures in larger groups of patients. We plan to use CA and HC to further investigate such perfusion patterns on both ictal and interictal SPECT data. Our method also could be applied to the analysis of other imaging modalities, such as FDG PET.

CONCLUSION

We propose a method to study the spatial statistical dependencies seen in SPECT brain perfusion data sets acquired from a homogeneous population of subjects. The method combines anatomical standardization analysis with correspondence analysis and ascending hierarchical clustering to explore relationships between perfusion profiles. We applied the method to normal SPECT images acquired from healthy subjects and ictal SPECT images acquired from patients with MTLE. Our results gave evidence of structured perfusion patterns involving four groups of anatomical regions: temporomesial structures, internal structures, posterior structures, and remaining cortex. Moreover, the temporal pole and lenticular nucleus seemed to be highly relevant to characterize ictal perfusion in patients with MTLE. The understanding of such spatial statistical dependency will certainly provide information regarding the underlying epileptogenic network.

ACKNOWLEDGMENT

The authors thank Dr Leighton Barnden (Woodville, Australia) for providing normal SPECT data and Dr Eliane Kobayashi (Montreal Neurological Institute, Canada) for fruitful discussion concerning the interpretation of results in the context of temporal lobe epilepsy.

REFERENCES

- Patterson J, Wyper DJ. Basics of SPECT. In: Duncan R, ed. *SPECT Imaging of the Brain*. Dordrecht, The Netherlands: Kluwer Academic, 1997; 1–42.
- Devous MD, Thisted RA, Morgan GF, Leroy RF, Rowe CC. SPECT brain imaging in epilepsy: a meta-analysis. *J Nucl Med* 1998; 39:285–293.
- Ho SS, Berkovic SF, McKay WJ, Kalnins RM, Bladin PF. Temporal lobe epilepsy subtypes: differential patterns of cerebral perfusion on ictal SPECT. *Epilepsia* 1996; 37:788–795.
- Chassoux F, Semah F, Boullieret V, et al. Metabolic changes and electro-clinical patterns in mesiotemporal lobe epilepsy: a correlative study. *Brain* 2004; 127:1–11.
- Lobaugh NJ, Caldwell CB, Black SE, Leibovitch FS, Swartz SH. Three brain SPECT region-of-interest templates in elderly people: normative values, hemispheric asymmetries, and a comparison of single- and multihead cameras. *J Nucl Med* 2000; 41:45–56.
- Van Laere K, Versijpt J, Audenaert K, et al. ^{99m}Tc -ECD brain perfusion SPET: variability, asymmetry and effect of age and gender in healthy adults. *Eur J Nucl Med* 2001; 28:873–887.
- Pagani M, Salmasso D, Jonsson C, et al. Regional cerebral blood flow assessment by principal component analysis and ^{99m}Tc -HMPAO SPET in healthy subjects at rest: normal distribution and effect of age and gender. *Eur J Nucl Med* 2002; 29:67–75.
- Grova C, Jannin P, Biraben A, et al. A methodology for generating normal and pathological brain perfusion SPECT images for evaluation of MRI/SPECT fusion methods: application in epilepsy. *Phys Med Biol* 2003; 48:4023–4043.
- Houston AS, Kemp PM, Macleod MA. A method for assessing the significance of abnormalities in HMPAO brain SPECT images. *J Nucl Med* 1994; 35:239–244.
- Blumenfeld H, McNally KA, Vanderhill SD, et al. Positive and negative network correlations in temporal lobe epilepsy. *Cerebr Cortex* 2004; 14:892–902.
- Stoeckel J, Malandain G, Migneco O, et al. Classification of SPECT images of normal subjects versus image of Alzheimer's disease patients. In: *Lecture Notes in Computer Science (MICCAI 2001, Utrecht)*. New York: Springer, 2001; 666–674.
- Chauvel P, Vignal JP, Biraben A, Badier JM, Scarabin JM. Stereoencephalography. In: Pawlik G, Stefan H, eds. *Multimethodological Assessment of the Epileptic Forms*. New York: Springer-Verlag, 1996; 80–108.
- Spencer SS. Neural networks in human epilepsy: evidence of and implications for treatment. *Epilepsia* 2002; 43:219–227.
- Shin WC, Hong SB, Tae WS, Seo DW, Kim SE. Ictal hyperperfusion of cerebellum and basal ganglia in temporal lobe epilepsy: SPECT subtraction with MRI coregistration. *J Nucl Med* 2001; 42:853–858.
- Sojkova J, Lewis PJ, Siegel AH, et al. Does asymmetric basal ganglia or thalamic activation aid in seizure foci lateralization on ictal SPECT studies? *J Nucl Med* 2003; 44:1379–1386.
- Lebart L, Morineau A, Warwick KM. *Multivariate Descriptive Statistical Analysis. Series in Probability and Mathematical Statistics*. New York: Wiley, 1984.
- Zubal IG, Harrell CR, Smith EO, Rattner Z, Gindi GR, Hoffer PB. Computerized three-dimensional segmented human anatomy. *Med Phys* 1994; 21:299–302.
- Engel J. *Surgical Treatment of the Epilepsies, volume 1*. New York: Raven Press, 1987.
- Jaszczak RJ, Floyd CE, Coleman RE. Scatter compensations techniques for SPECT. *IEEE Trans Nucl Sci* 1985; 32:786–793.
- Chang L-T. A method for attenuation correction in radionuclide computed tomography. *IEEE Trans Nucl Sci* 1978; NS-25:638–643.
- Friston KJ, Ashburner J, Poline JB, Frith CD, Heather JD, Frackowiak RSJ. Spatial registration and normalization of images. *Hum Brain Mapp* 1995; 2:165–189.
- Acton PD, Friston KJ. Statistical parametric mapping in functional neuroimaging: beyond PET and fMRI activation studies. *Eur J Nucl Med* 1998; 25:663–667.
- Maes F, Collignon A, Vandermeulen D, Marchal G, Suetens P. Multimodality image registration by maximization of mutual information. *IEEE Trans Med Imaging* 1997; 16:187–198.
- Soret M, Koulibaly PM, Darcourt J, Hapdey S, Buvat I. Quantitative accuracy of dopaminergic neurotransmission imaging with ^{123}I SPECT. *J Nucl Med* 2003; 44:1184–1193.
- Frouin V, Comtat C, Reilhac A, Grégoire M-C. Correction of partial-volume effect for PET striatal imaging: fast implementation and study of robustness. *J Nucl Med* 2002; 43:1715–1726.
- Matsuda H, Ohnishi T, Asada T, et al. Correction for partial-volume effects on brain perfusion SPECT in healthy men. *J Nucl Med* 2003; 44:1243–1252.
- Hellier P, Ashburner J, Corouge I, Barillot C, Friston KJ. Inter-subject registration of functional and anatomical data using SPM. In: *Lecture Notes in Computer Science (MICCAI 2002, Tokyo)*. Berlin: Springer-Verlag, 2002; 590–597.
- Stamatakis EA, Wilson JTL, Wyper DJ. Spatial normalization of lesioned HMPAO SPECT images. *Neuroimage* 2001; 14:844–852.
- Grova C, Jannin P, Buvat I, Benali H, Gibaud B. Evaluation of registration of ictal SPECT/MRI data using statistical similarity methods. In: *Lecture Notes in Computer Science: MICCAI 2004, Saint Malo, volume 3216*. New York: Springer, 2004; 687–695.
- Collins DL, Zijdenbos AP, Baaré WF, Evans AC. ANIMAL+ INSECT: Improved cortical structure segmentation. In: *Proceedings of Information Processing in Medical Imaging IPMI'99*. Berlin: Springer-Verlag GmbH, 1999; 210–223.
- Newton MR, Berkovic SF, Austin MC, Reutens DC, McKay WJ, Bladin PF. Dystonia, clinical lateralization, and regional blood flow changes in temporal lobe seizures. *Neurology* 1992; 42:371–377.

32. Dupont S, Semah F, Baulac M, Samson Y. The underlying pathophysiology of ictal dystonia in temporal lobe epilepsy: an FDG-PET study. *Neurology* 1998; 51:1289–1292.
33. Bouilleret V, Valenti MP, Hirsch E, Semah F, Namer IJ. Correlation between PET and SISCOM in temporal lobe epilepsy. *J Nucl Med* 2002; 43:991–998.
34. Ryvlin P, Kahane P, Arzimanoglou A, Andermann F, eds. *Epileptic Disorders: Temporal Pole and Mesiotemporal Epilepsy*, volume 4 (Suppl 1). John Libbey Eurotext, 2002.
35. Coste S, Ryvlin P, Hermier M, et al. Temporopolar changes in temporal lobe epilepsy: a quantitative MRI-based study. *Neurology* 2002; 59: 855–861.
36. Bartolomei F, Wendling F, Vignal J-P, et al. Seizures of temporal lobe epilepsy: identification of subtypes by coherence analysis using stereo-electro-encephalography. *Clin Neurophysiol* 1999; 110:1741–1754.
37. Norden AD, Blumenfeld H. The role of subcortical structures in human epilepsy. *Epilepsy Behav* 2002; 3:219–231.